Directional Emittance of a Two-Dimensional Scattering Medium with Fresnel Boundaries

C. Y. Wu,* W. H. Sutton,† and T. J. Love‡
University of Oklahoma, Norman, Oklahoma

The influences of the refractive index, scattering albedo, and optical sizes on the thermal radiation in a two-dimensional rectangular, isotropically scattering medium bounded by optically smooth boundaries having Fresnel reflection are considered. The complexity of formulation resulting from this specular reflection is reduced by treating the images as effective media and by neglecting the radiation from faraway images. The problem can then be described by an integral equation (the source function) that is solved iteratively here; the method is then applied to study the directional emittance of a two-dimensional semi-infinite slab. Results show that the directional emittance is azimuthally dependent for the rectangular geometries, that the effects of the relative refractive index on the emittance depend significantly on the albedo, and that Fresnel reflection generally decreases the angular dependence of the emittance compared to free boundaries.

Nomenclature

I = dimensionless intensity of radiation defined in Eq. (4)
I^* = intensity of radiation
I_b^* = Planck function for emission
n = relative refractive index, i.e., refractive index relative to surroundings
r = radius or optical distance defined in Eq. (23)
R = distance defined in Eq. (27)
$\mathbf{r}$ = position vector
s = dimensionless optical coordinate along a ray, Eq. (3)
$\mathbf{s}$ = unit vector on the path of a ray
s_0 = length of an optical path
s^* = optical coordinate along a ray
S = dimensionless source function defined in Eq. (4)
S^* = source function defined in Eq. (2)
β^* = extinction coefficient
Δr_m = defined in Eq. (20), $m = 1, 2, 3, 4$
θ = polar angle
θ_{cr} = critical angle defined in Eq. (14)
θ_n = angle relative to the normal of a surface, Eqs. (15) and (16)
κ^* = absorption coefficient
ρ = reflectivity of an interface or its image, Eq. (13)
σ^* = scattering coefficient
ϕ = azimuthal angle
ω = scattering albedo
$d\Omega$ = differential solid angle
$\mathbf{\Omega}$ = unit vector along the path of ray

Introduction

ALTHOUGH a considerable amount of work has been done in both multidimensional radiative transfer in a scattering medium[1-22] and in slab problems dealing with Fresnel reflectance,[23-27] little work has been done on multidimensional Fresnel problems.[1,19,20] Recently, numerous papers dealing with anisotropic scatter effects[2,7,12,14] have been published in the literature. The effects of Fresnel reflectance may give a similar type of distribution, depending on the geometry and on incident radiation.

Here, we seek to demonstrate a method for handling Fresnel reflectance in a multidimensional setting. Such problems are very important in situations such as melting, where the melt has properties somewhat different from the solid, and problems with laser interaction with solids, where the direction of the external radiation or orientation of the boundary may be far more significant than the internal scattering properties.

The particular problems considered here are solvable by Monte Carlo methods. Turner and Love[19] analyzed directional emittance of a two-dimensional coating with Fresnel reflection at the boundaries. However, the Monte Carlo method is very laborious and time consuming. Therefore, to solve this type of problem combined with conduction or in a more "realistic" setting (that is, with more parameters to study), a more effective method of analysis is necessary.

There are several possible two-dimensional problems that can be solved, as illustrated in Fig. 1. One is a quarter space, that is, two perpendicular boundaries extending to infinity. Another case is a truncated two-dimensional slab. We refer to this as a semi-infinite plate. A third is an infinite rectangular bar geometry. Here, we will consider the formulation of an analysis suitable for all three cases from the perspective of Fresnel reflectance. The example of the quarter space will be explicitly analyzed for illustration purposes. Results will be presented for directional emittance of the semi-infinite plate.

Several alternative methods exist for solving this type of problem. One method is to solve the radiative transfer equation directly by whatever means, some of which include discrete ordinates, multiflux methods, spherical harmonics methods, or Monte Carlo methods. In two dimensions, the problem requires at least two spatial and two angular dimensions. Here, in the case of isotropic scattering, we require only the two spatial dimensions since we will deal with the integral form of the radiative transfer equation.

The method we have chosen to use is an iterative method for the various interactions of multiple reflections. The boundary reflectances are handled by imaging, that is, as in nonparticipating media, where multiple reflections can be observed by ray-tracing methods. Here, we will take a similar approach, Also, we will truncate the solution after a certain number of multiple reflections, much as a Monte Carlo solution would trace a ray through a certain number of interactions until the beam is extinguished.

Received Sept. 2, 1987; revision received June 9, 1988.

*Associate Professor, School of Aerospace, Mechanical and Nuclear Engineering (permanently with Department of Mechanical Engineering, National Cheng Kung University, Tainan, Taiwan).

†Assistant Professor, School of Aerospace, Mechanical and Nuclear Engineering. Member AIAA.

‡Professor, School of Aerospace, Mechanical and Nuclear Engineering. Associate Fellow AIAA.

Formulation

In the presence of Fresnel reflection at the boundaries, the rectangular bar and the semi-infinite slab both have an infinite number of images (Figs. 1b and 1c); the quarter space has only three images (Fig. 1a). Thus, mathematically, the formulation for the radiative transfer in a quarter space is the simplest one among two-dimensional rectangular geometries. For this reason, this case is chosen to explain the method of formulation used in this work.

In general, the radiative intensity I^* along a path s^* in a participating medium is governed by the transport equation in the direction $\mathbf{\Omega}$,

$$\frac{dI^*(s^*)}{ds^*} + \beta^* I^*(s^*) = \beta^* S^*(s^*) \tag{1}$$

where β^* is the extinction coefficient defined as the sum of the scattering coefficient σ^* and the absorption coefficient κ^*, $\mathbf{\Omega}$ the direction defined by a polar angle θ and an azimuthal angle ϕ, and S^* the source function. For a medium that emits, absorbs, and isotropically scatters radiation, the source function is defined as

$$S^*(s^*) = (1-\omega)n^2 I_b^*(s^*) + \frac{\omega}{4\pi}\int_{4\pi} I^*(s^*,\mathbf{\Omega}')\, d\Omega' \tag{2}$$

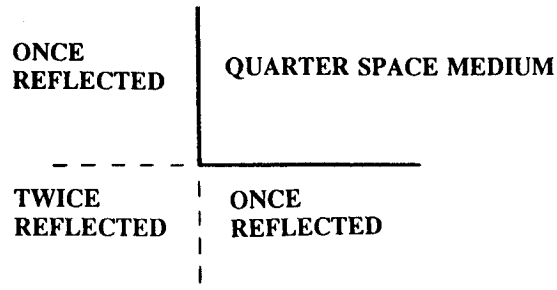

a) Quarter space, finite images

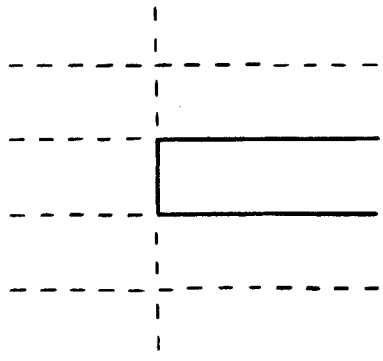

b) Semi-infinite slab, infinite images about plane of symmetry

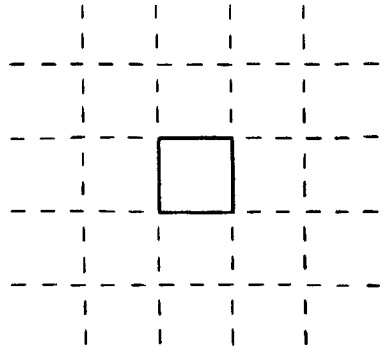

c) Infinite bar, infinite images

Fig. 1 Possible two-dimensional rectangular geometries, illustrating reflected images.

where I_b^* is the Planck function for emission and ω the scattering albedo defined as the scattering coefficient divided by the extinction coefficient.

Since Crosbie and Schrenker[5] have derived exact expressions for the radiative transfer in a rectangular medium without considering boundary reflection, the present work aims to consider a more general integral equation for the radiative transfer in a rectangular medium with Fresnel reflection at the boundaries. The resultant integral equation for a quarter space is shown here. Details of other situations are excluded at this time, but follow the same type of formulation.[20]

For directional emittance, we assume that the medium in the quarter space is homogeneous, isothermal, and not subjected to external radiation and that the refractive index of the medium relative to that of surroundings is n. Defining dimensionless quantities

$$s = \beta^* s^* \tag{3}$$

$$I = \frac{I^*}{n^2 I_b^*} \tag{4}$$

$$S = \frac{S^*}{n^2 I_b^*} \tag{5}$$

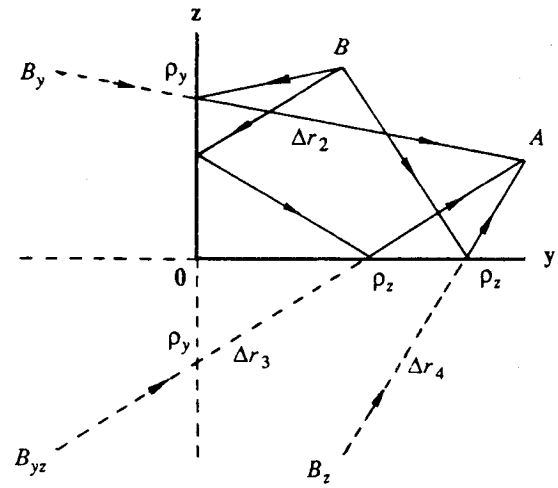

a) Three-dimensional radiation path

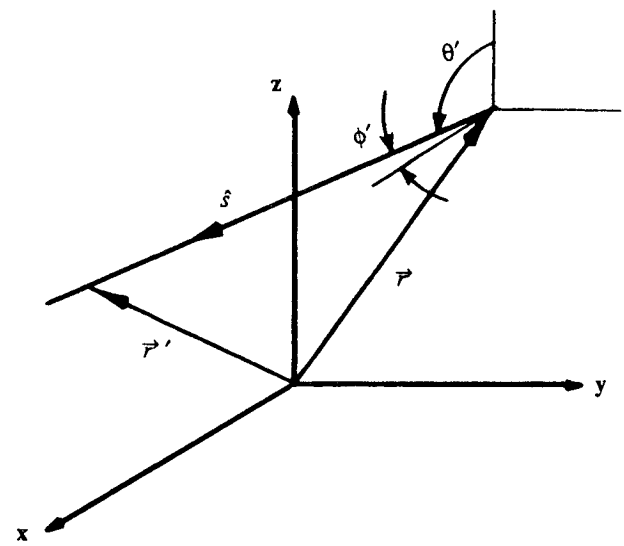

b) Images of B viewed from A, planar projection

Fig. 2 Radiation path geometry.

In Cartesian coordinates, Eqs. (1) and (2) become

$$\sin\theta\sin\phi\frac{\partial I(y,z,\theta,\phi)}{\partial y}+\cos\theta\frac{\partial I(y,z,\theta,\phi)}{\partial z}+I(y,z,\theta,\phi)=S(y,z) \tag{6}$$

and

$$S(y,z)=(1-\omega)+\frac{\omega}{4\pi}\int_0^{\pi}\int_0^{2\pi} I(y,z,\theta',\phi')\sin\theta'\,d\phi'\,d\theta' \tag{7}$$

where $0\le y$, $0\le z$, $0\le\theta\le\pi$, and $0\le\phi<2\pi$, shown in Fig. 2b. Referring to Fig. 2a, the radiant energy transferred from an element of the medium at point B to an element of the medium at point A includes the radiant energy transferred directly through the realistic medium and that transferred from B to A by the reflection at the mirrorlike boundaries. The indirect transfer of energy may be treated as the transfer of energy from the images of sources, such as B_y, B_z, and B_{yz} in Fig. 2a, to the receptor. However, the reflection is usually not complete and the optical path of the transfer by the reflection is longer than that of the direct transfer, as shown in the figure. Based on the concept of images, the effective medium that transfers energy to the receptor at point A in the realistic medium shall include the images due to Fresnel reflection at the boundaries. The indirect transfer of radiant energy from images may take the place of boundary conditions in the present procedure of formulation. Then, the formal solution of an intensity in the direction (θ,ϕ) at a point (y,z) may be expressed in terms of the source function in the effective medium as:

$$I(x,y,\theta,\phi)=\int_0^{z/\cos\theta'} S(s')e^{-s'}\,ds'$$

$$+\int_{z/\cos\theta'}^{y/\sin\theta'\sin\phi'} \rho_z(\theta')S(s')e^{-s'}\,ds'$$

$$+\int_{y/\sin\theta'\sin\phi'}^{\infty} \rho_z(\theta')\rho_y(\theta',\phi')S(s')e^{-s'}\,ds'$$

with

$$\theta'=\theta \text{ and } \phi'=\phi \text{ for } 0\le\theta\le\tan^{-1}(y/z\sin\phi)$$

and

$$0\le\phi\le\pi/2 \tag{8}$$

$$I(y,z,\theta,\phi)=\int_0^{y/\sin\theta'\sin\phi'} S(s')e^{-s'}\,ds'$$

$$+\int_{y/\sin\theta'\sin\phi'}^{z/\cos\theta'} \rho_y(\theta',\phi')S(s')e^{-s'}\,ds'$$

$$+\int_{z/\cos\theta'}^{\infty} \rho_z(\theta')\rho_y(\theta',\phi')S(s')e^{-s'}\,ds'$$

with

$$\theta'=\theta \text{ and } \phi'=\phi \text{ for } \tan^{-1}(y/z\sin\phi)\le\theta\le\pi/2$$

and

$$0\le\phi\le\pi/2 \tag{9}$$

$$I(y,z,\theta,\phi)=\int_0^{y/\sin\theta'\sin\phi'} S(s')e^{-s'}\,ds'$$

$$+\int_{y/\sin\theta'\sin\phi'}^{\infty} \rho_y(\theta',\phi')S(s')e^{-s'}\,ds'$$

with

$$\theta'=\pi-\theta \text{ and } \phi'=\phi \text{ for } \pi/2<\theta\le\pi,\ 0\le\phi\le\pi/2 \tag{10}$$

$$I(y,z,\theta,\phi)=\int_0^{\infty} S(s')e^{-s'}\,ds'$$

for

$$\pi/2<\theta\le\pi,\ 3\pi/2\le\phi<2\pi \tag{11}$$

$$I(y,z,\theta,\phi)=\int_0^{z/\cos\theta'} S(s')e^{-s'}\,ds'+\int_{z/\cos\theta'}^{\infty} \rho_z(\theta')S(s')e^{-s'}\,ds'$$

with

$$\theta'=\theta \text{ for } 0\le\theta\le\pi/2,\ 3\pi/2\le\phi<2\pi \tag{12}$$

where $s'=[x'^2+(y'-y)^2+(z'-z)^2]^{\frac{1}{2}}$, ρ_z is the reflectivity at a x–y surface and its images, and ρ_y is the reflectivity at a z–x surface and its images. Because of the symmetry of the radiative field, the same expressions also hold in the other side of y–z plane. The reflectivity is given by the Fresnel equation[28] as

$$\rho=\frac{1}{2}\left\{\left[\frac{(1-n^2\sin^2\theta_n)^{\frac{1}{2}}-n\cos\theta_n}{(1-n^2\sin^2\theta_n)^{\frac{1}{2}}+n\cos\theta_n}\right]^2\right.$$

$$\left.+\left[\frac{\cos\theta_n-n(1-n^2\sin^2\theta_n)^{\frac{1}{2}}}{\cos\theta_n-n(1+n^2\sin^2\theta_n)^{\frac{1}{2}}}\right]^2\right\}^{\frac{1}{2}} \quad \theta_n\le\theta_{cr} \tag{13a}$$

$$\rho=1, \quad \theta_n>\theta_{cr} \tag{13b}$$

where

$$\theta_{cr}=\sin^{-1}(1/n) \tag{14}$$

$$\theta_n=\theta_y=\cos^{-1}(\sin\theta\sin\phi) \quad \text{at } z\text{–}x \text{ boundaries} \tag{15}$$

$$\theta_z=\theta \quad \text{at } x\text{–}y \text{ boundaries} \tag{16}$$

For convenience, we write ρ as $\rho_y(\theta,\phi)$ at the interfaces normal to the y axis and ρ as $\rho_z(\theta)$ at the interfaces normal to the z axis. When $n=1$, ρ reduces to zero.

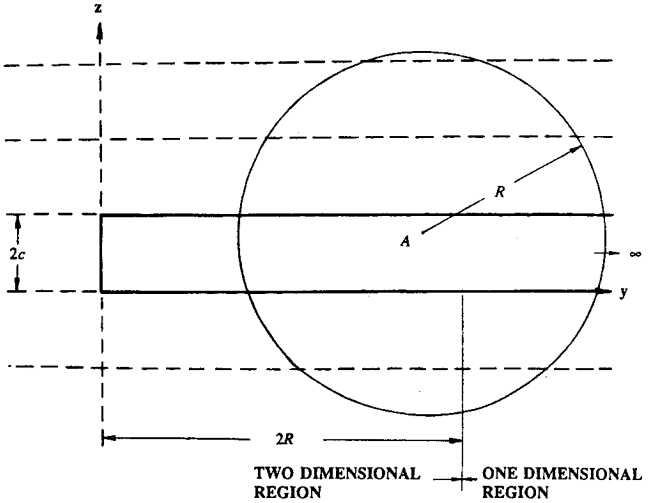

Fig. 3 Two- and one-dimensional subregion.

Expressions identical to Eqs. (8–12) can also be obtained by an extension of Smith's method of split intensities.[17,18] However, the extension of Smith's method is much more complicated than the present method.[20]

Substitution of Eqs. (8–12) into Eq. (7) produces

$$
\begin{aligned}
S(y,z) = (1-\omega)\\
&+\frac{\omega}{2\pi}\int_{\phi'=0}^{\pi/2}\left\{\int_{\theta'=0}^{\tan^{-1}(y/z\sin\phi')}\sin\theta'\left[\int_0^{z/\cos\theta'} S(s')e^{-s'}\,ds'\right.\right.\\
&+\int_{z/\cos\theta'}^{y/\sin\theta'\sin\phi'}\rho_z(\theta')S(s')e^{-s'}\,ds'\\
&\left.+\int_{y/\sin\theta'\sin\phi'}^{\infty}\rho_z(\theta')\rho_y(\theta',\phi')S(s')e^{-s'}\,ds'\right]d\theta'\\
&+\int_{\tan^{-1}(y/z\sin\phi')}^{\pi/2}\sin\theta'\left[\int_0^{y/\sin\theta'\sin\phi'} S(s')e^{-s'}\,ds'\right.\\
&+\int_{y/\sin\theta'\sin\phi'}^{z/\cos\theta'}\rho_y(\theta',\phi')S(s')e^{-s'}\,ds'\\
&\left.+\int_{z/\cos\theta'}^{\infty}\rho_z(\theta')\rho_y(\theta',\phi')S(s')e^{-s'}\,ds'\right]d\theta'\\
&+\int_{\theta'=0}^{\pi/2}\sin\theta'\left[\int_0^{y/\sin\theta'\sin\phi'} S(s')e^{-s'}\,ds'\right.\\
&\left.+\int_{y/\sin\theta'\sin\phi'}^{\infty}\rho_y(\theta',\phi')S(s')e^{-s'}\,ds'\right]d\theta'\\
&+\int_{\theta'=0}^{\pi/2}\sin\theta'\int_0^{\infty} S(s')e^{-s'}\,ds'\,d\theta'\\
&+\int_{\theta'=0}^{\pi/2}\sin\theta'\left[\int_0^{z/\cos\theta'} S(s')e^{-s'}\,ds'\right.\\
&\left.\left.+\int_{z/\cos\theta'}^{\infty}\rho_z(\theta')S(s')e^{-s'}\,ds'\right]d\theta'\right\}d\phi' \qquad (17)
\end{aligned}
$$

Next, by following a procedure similar to Crosbie and Schrenker,[5] the integrals over paths and solid angles may be transferred into volume integrals. Figure 2b shows an arbitrary path from point B in the effective medium, where the effective source is located, to point A in the realistic medium, where the studied point is located. For the path, $s' = \boldsymbol{s}\cdot(\boldsymbol{r}'-\boldsymbol{r})$ and, at point B, $ds'\,d\Omega' = dV'/|\boldsymbol{r}'-\boldsymbol{r}|^2$, where dV' is the element of volume at point B and $d\Omega' = \sin\theta'\,d\theta'\,d\phi'$. Using

$$|\boldsymbol{r}'-\boldsymbol{r}| = [(x'-x)^2+(y'-y)^2+(z'-z)^2]^{\frac{1}{2}}$$

then,

$$\frac{dV'}{|\boldsymbol{r}'-\boldsymbol{r}|^2} = \frac{dx'\,dy'\,dz'}{[(x'-x)^2+(y'-y)^2+(z'-z)^2]}$$

In the present analysis, $x = 0$. Then, Eq. (14) is transformed into

$$
\begin{aligned}
S(y,z) = (1-\omega)\\
&+\frac{\omega}{2\pi}\int_0^{\infty}\int_0^{\infty} S(y',z')\int_0^{\infty}\left[\frac{e^{-\Delta r_1}}{(\Delta r_3)^2}\right.\\
&+\rho(\theta_{2y})\frac{e^{-\Delta r_2}}{(\Delta r_2)^2}+\rho(\theta_{3y})\rho(\theta_{3z})\frac{e-\Delta r_3}{(\Delta r_3)^2}\\
&\left.+\rho(\theta_{4z})\frac{e^{-\Delta r_4}}{(\Delta r_4)^2}\right]dx'\,dy'\,dz' \qquad (18)
\end{aligned}
$$

where

$$
\begin{aligned}
\theta_{2y} &= \cos^{-1}[(y+y')/(\Delta r_2)]\\
\theta_{3y} &= \cos^{-1}[(y+y')/(\Delta r_3)]\\
\theta_{3z} &= \cos^{-1}[(z+z')/(\Delta r_3)]\\
\theta_{4z} &= \cos^{-1}[(z+z')/(\Delta r_4)] \qquad (19)
\end{aligned}
$$

$$
\begin{aligned}
\Delta r_1 &= [(0-x')^2+(y-y')^2+(z-z')^2]^{\frac{1}{2}}\\
\Delta r_2 &= [(0-x')^2+(y+y')^2+(z-z')^2]^{\frac{1}{2}}\\
\Delta r_3 &= [(0-x')^2+(y+y')^2+(z+z')^2]^{\frac{1}{2}}\\
\Delta r_4 &= [(0-x')^2+(y-y')^2+(z+z')^2]^{\frac{1}{2}} \qquad (20)
\end{aligned}
$$

In Fig. 2a, the effective sources B_y, B_{yz}, B_z are the images of the source at B and their optical distances to A are Δr_2, Δr_3, and Δr_4, respectively. Note that the four integration terms in Eq. (18) have similar form, but the last three terms contain the Fresnel reflectivities and longer optical distances. The construction of Eq. (18) suggests a more straightforward procedure to derive the equation of radiative transfer as outlined in the following:

1) Draw a figure containing a sufficient number of images resulting from Fresnel reflection and construct the effective optical coordinates and the effective optical distance for the effective source in each image, for example, $(x', -y', z')$ and Δr_2, $(x', -y', -z')$ and Δr_3, and $(x', y', -z')$ and Δr_4 for B_y, B_{yz}, and B_z in Fig. 2a, respectively.

2) Derive the integral equation of radiative transfer without considering the reflection at the boundaries and, next, for every image, construct the integration term for the image, whose integration domain and integrand are identical to those of the integration term for the direct radiative transfer, except that the integrand contains reflectivities for Fresnel reflection at the boundaries and the optical distance between the effective source and the point studied takes the place of the optical distance for the direct radiative transfer.

3) Add the integration terms for all images to the right-hand side of the integral equation for the radiative transfer without considering reflecting boundaries to obtain the final integral equation.

As noted previously, if more than two of the boundaries of the medium have Fresnel reflection, the effective medium contains an infinite number of images. Since the contribution of each image to the source function is represented by an integration term in the integral equation of radiative transfer, the integral equation of this problem has an infinite number of integration terms. Thus, the solution of this equation appears formidable, if not impossible. Fortunately, if the radiation from the effective medium outside a large sphere with center at A and a radius R, as shown in Fig. 3, is small enough, then only a small number of integration terms representing the incident radiation on A from the effective medium

inside the sphere are important for the solution. Therefore, by neglecting the radiation from the effective medium outside the sphere with a large radius equal to R, a relevant simplification of computation may be obtained.

The upper bound (ub) of the total contribution of the effective medium at $r > R$ to the source function and the minimum value of the source function is conservatively assessed, producing an upper bound of relative error caused by the neglect of radiation from the effective medium at $r > R$, $(E_r)_{ub}$, which is a function of R. Alternatively, R may be expressed as a function of $(E_r)_{ub}$. Therefore, R can be determined from the accuracy required or the relative error due to the simplification can be controlled directly.

Extension to the Semi-Infinite Slab

Consider a semi-infinite isothermal slab that absorbs, emits, and isotropically scatters thermal radiation, as shown in Fig. 1b. The same assumptions applied to the quarter space problem apply here. Although the properties of the medium are dependent on the frequency of radiation, the use of a frequency subscript has been omitted in the following formulation to simplify the mathematical expressions.

From the previous discussion, we know that the effective medium for the present system includes a realistic medium, its image in the y direction, and an infinite number of images in the z direction, as shown in Fig. 1b. Then, by the same procedure, the integral equation for the present problem may be written as

$$S(y,z) = 1 - \omega + \omega \sum_{p=-1}^{0} \sum_{q} S_{pq}(y,z) \tag{21}$$

where $0 \le y < \infty$, $0 \le z \le 2c$ and

$$S_{pq}(y,z) = \frac{1}{2\pi} \int_0^{2c} \int_0^{\infty} S(y',z') \int_0^{\infty} \rho\left[\cos^{-1}\left(\frac{\Delta y_p}{r_{pq}}\right)\right]^{|p|} \times \rho\left[\cos^{-1}\left(\frac{\Delta z_q}{r_{pq}}\right)\right]^{|q|} \frac{e^{-r_{pq}}}{r_{pq}^2}\, dx'\, dy'\, dz' \tag{22}$$

with

$$q = \text{any integer}$$

$$r_{pq} = [(\Delta x)^2 + (\Delta y_p)^2 + (\Delta z_q)^2]^{\frac{1}{2}} \tag{23}$$

$$\Delta x = |x' - 0| \tag{24}$$

$$\Delta y_p = |y - y'|, \quad \text{for } p = 0$$
$$y + y', \quad \text{for } p = -1 \tag{25}$$

and

$$\Delta z_q = 2c - z + 2c \cdot \text{mod}(q,2) + (-1)^{\text{mod}(q,2)} z' + 2c(q-1), \quad \text{for } q > 0$$
$$= |z - z'|, \quad \text{for } q = 0$$
$$= z + 2c \cdot \text{mod}(1 + |q|,2) + (-1)^{\text{mod}(1+|q|,2)} z' + 2c(-q-1), \quad \text{for } q < 0 \tag{26}$$

where mod$(q,2)$ in Eq. (26) is defined as

$$\text{mod}(q,2) = q - \text{integral part of } q/2$$

At this point, a very important practical facet of this work should be pointed out. The radiation exchange between any two points separated by $r \ge R$, where

$$R = \ell n \left[\frac{\omega}{(1-\omega)(E_r)_{ub}}\right] \tag{27}$$

is negligible, provided that $(E_r)_{ub}$ is small enough.[20]

$(E_r)_{ub}$ in Eq. (27) is the maximum tolerant error incurred by neglecting radiation from the effective medium at $r \ge R$. In order to simplify the evaluation of the extremely complicated integration terms on the right-hand side of Eq. (21), $(E_r)_{ub}$ is chosen as 10^{-3} and the contribution of the effective medium at $r \ge R$, where

$$R = \ell n \left[\frac{\omega}{0.001(1-\omega)}\right]$$

to the point studied is neglected. In addition, for the same reason, the effects of the edge (at $y = 0$), on the medium far from the edge is negligible. That is, the radiative transfer in the medium far away from the edge appears to be one-dimensional. In this analysis, it is conservatively assumed that the radiative transfer in the region $0 \le y \le 2R$ is two-dimensional and the radiative transfer in the region $y > 2R$ is one-dimensional to account for reflection along the infinite y direction.

Numerical iteration is used to solve the resultant integral equation. Numerical techniques of integration discussed by Crosbie and Schrenker[6] and iteration are employed in this work. In order to increase the accuracy of the numerical integration, Gaussian quadrature formula is used instead of the Labatto quadrature formula used by Crosbie and Schrenker.[6] The nonintegration term on the right-hand side of Eq. (21), $1 - \omega$, is used as the initial guess for iteration. When the maximum difference between the source functions obtained in two successive iterations is less than 10^{-3}, it is found that the source function for y close to $2R$ agrees with that in the one-dimensional region to at least three digits for the cases studied in this work. Therefore, when the maximum difference between the source functions obtained in two successive iterations is less than 10^{-3}, the solution is assumed to be convergent in this analysis.

After obtaining the source function, the radiative intensity may be obtained by the integration of the transport equation. The directional emittance for the slab can be related to the intensity inside the medium by

$$\varepsilon(y,2c,\theta',\phi') = [1 - \rho_z(\theta)] I(y,2c,\theta,\phi) \tag{28}$$

at the top surface and

$$\varepsilon(0,z,\theta',\phi') = [1 - \rho_y(\theta,\phi)] I(0,z,\theta,\phi) \tag{29}$$

at the edge surface, where (θ,ϕ) and (θ',ϕ') are related by Snell's law and I is the dimensionless intensity defined in Eq. (4).

Results and Discussion

The radiative transfer in a participating medium with Fresnel reflection at the boundaries is characterized by the refractive index, the scattering albedo, and the optical thickness of the medium. The directional emittance of a semi-infinite slab is a function of the location (y,z) and the direction (θ,ϕ).

For purpose of comparison, the normal emittance for two different optical thicknesses, $2c = 5.0$ and 3.0, and various albedos obtained by this work and that by Turner and Love[19] are shown in Figs. 4 and 5. The agreement with Turner and Love's data is very good. The maximum difference is about 5% for $\omega = 0.95$ and $2c = 3.0$, occurring at the corners. In the absence of more precise comparisons, it is reasonable to conclude that the current formulation is valid.

From Figs. 4a and 5b, it is found that the plane normal emittance from the top surface of a semi-infinite slab approaches that from the top surface of an infinite slab at some distance away from the edge surface. The distance increases as the scattering albedo increases. This is because a larger scattering albedo represents a relatively weaker absorption and thus requires a longer optical path to approach the infinite limit.

The angular dependence of the directional emittance at various locations is shown for three optical thicknesses, $2c = 1.0$, 3.0 and 5.0, a scattering albedo, $\omega = 0.95$ and 0.99, and a refractive index, $n = 1.4$, in Figs. 6–8. The plane directional emittance is larger for an interface position located at a farther distance from the corners. The edge directional emittance at $z = c$ on the edge surface is always larger than that at the other locations. These results are caused by the effects of the corners. The angular distribution of the plane emittance from the top surface of a semi-infinite slab at $y = 4.5$ is very similar to that of the emittance from the top surface of an infinite slab. Moreover, as might be expected, the azimuthal dependence disappears for locations far away from the edge surface. Thus, it may be concluded that the infinite limit is approached as y becomes larger and larger.

A significant dependence of the plane directional emittance on azimuthal angles is found for the locations close to the corners, as shown in Figs. 9 and 10. In addition, the dependence of the plane directional emittance on polar angles appears to have a similar distribution for various albedos and optical thicknesses, provided that the directional emittance curves are at the same location and on the same view plane. The large drop in the magnitude of the directional emittance near 90 deg from the normal line of an interface is because near the critical angle the interface reflectivity increases rapidly. The strong dependence of the emittance on azimuthal angles requires the directional emittance to be shown on many different view planes. Thus, the figures shown in this two-dimensional analysis are far more than those in one-dimensional analyses. Each of Figs. 6–8 includes the directional emittance on four view planes. The curves of directional emittance from points on the top surface do not have symmetry, except those on the view planes parallel to the edge surface, and become more unsymmetrical as the view plane becomes closer to the plane at $y = 0$. Furthermore, for the radiation rays with the same polar angle, the ray in the direction leaving the edge surface has a longer optical path and fewer opportunities through the interfaces, so the emittance $\varepsilon(\theta,\phi)$ in the direction leaving the edge surface is greater than the emittance $\varepsilon(\theta,\phi - \pi)$. The curves of the edge emittance have the shape and trend similar to those of the plane emittance. That is, the symmetry of the emittance curves holds only on the view planes parallel to the top surface or containing the centerline of the edge surface, the emittance curves

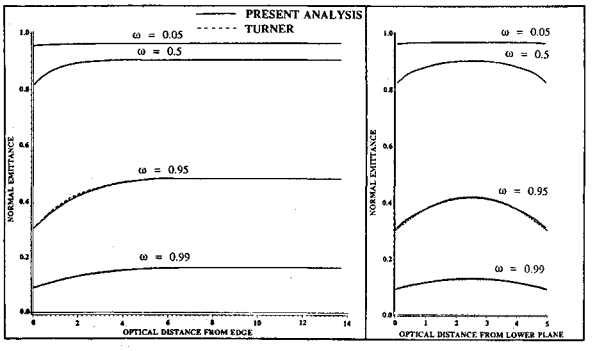

a) Top surface b) Edge surface

Fig. 4 Normal emittance for various albedos: $n = 1.4$, $2c = 5.0$.

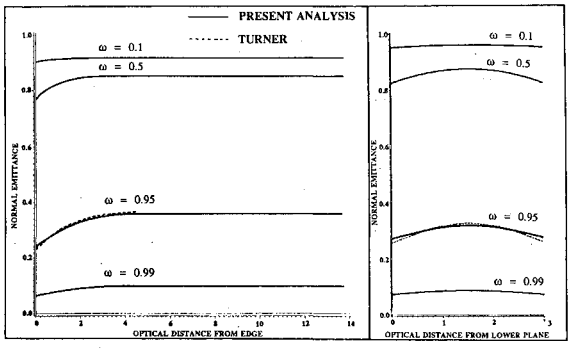

a) Top surface b) Edge surface

Fig. 5 Normal emittance for various albedos: $n = 1.4$, $2c = 3.0$.

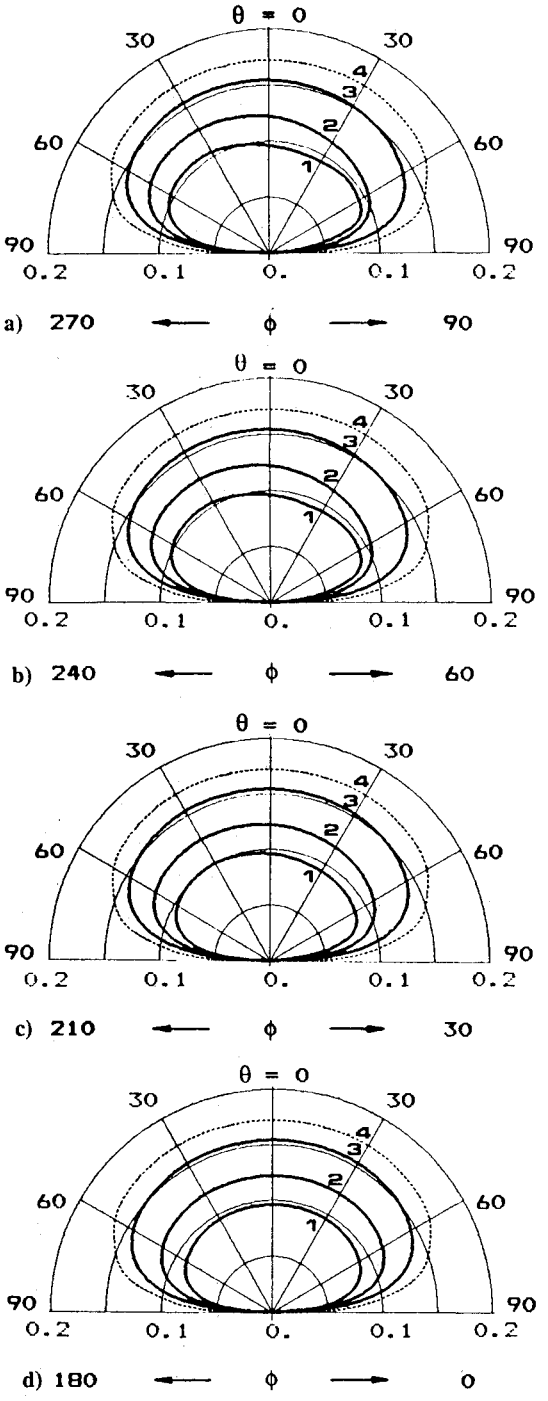

Fig. 6 Directional emittance for various positions on the top surface: $n = 1.4$, $\omega = 0.99$, $2c = 5.0$; curve 1 for points at $y = 0.3$, curve 2 for points at $y = 1.5$, curve 3 for points at $y = 4.5$, curve 4 for one-dimensional solution.

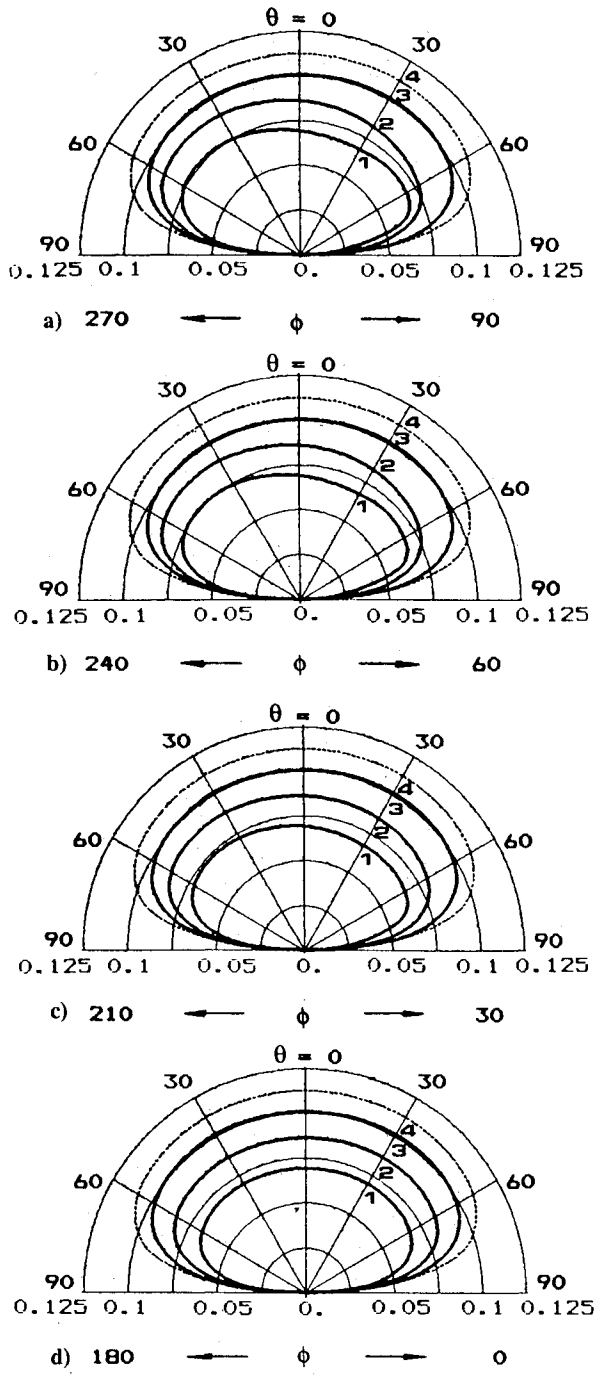

Fig. 7 Directional emittance for various positions on the top surface: $n = 1.4$, $\omega = 0.99$, $2c = 3.0$; curve 1 for points at $y = 0.3$, curve 2 for points at $y = 1.5$, curve 3 for points at $y = 4.5$, curve 4 for one-dimensional solution.

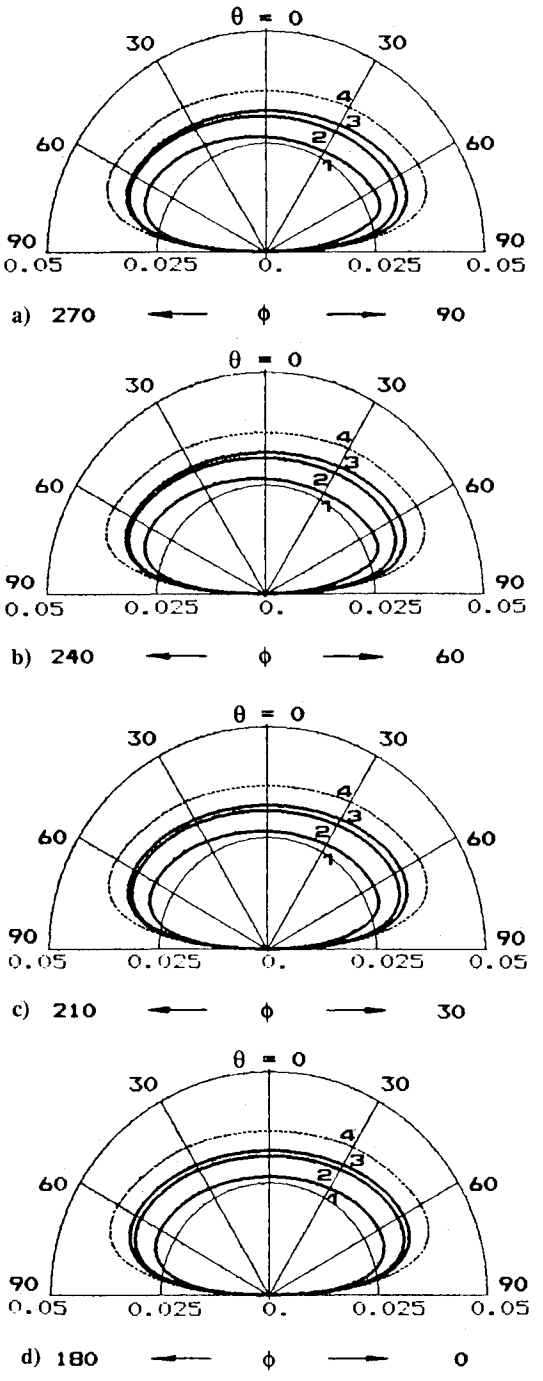

Fig. 8 Directional emittance for various positions on the top surface: $n = 1.4$, $\omega = 0.99$, $2c = 1.0$; curve 1 for points at $y = 0.3$, curve 2 for points at $y = 1.5$, curve 3 for points at $y = 4.5$, curve 4 for one-dimensional solution.

become more unsymmetrical as the view plane is located closer to the corners, and, on the same view plane, the larger of the emitted radiation intensities with the same angle from the line normal to the edge surface is in the direction leaving the top or the bottom surface.

The effects of the refractive index on the emittance depend on the scattering albedo, as shown in Fig. 11. An increase in the refractive index reduces the emittance for a weakly scattering medium, for example, $\omega = 0.1$ in Fig. 11. However, for a strongly scattering medium, for example, $\omega = 0.9$ in that figure, the reverse is true. This is because a larger refractive index causes more energy to be reflected internally and a smaller albedo causes more energy to be absorbed. That is, more energy is absorbed in a medium with a smaller albedo and a larger refractive index. However, when the albedo is larger, more reflection increases the effects of scattering and thus increases the emittance. Since Turner had studied only the emittance for $\omega = 0.95$ and 0.99, he did not recognize the variation of the emittance with the refractive index for a weakly scattering medium.[4] For $\omega = 0.9$ and $2c = 3.0$, the variation of the directional emittance with different refractive indexes are shown in Figs. 12 and 13. It is found that the variation of the emittance with the refractive index is nonlinear and the shape of curves is the same for $n = 1.4$ and 1.8. Turner's and Bobco's results[1,19] for $n = 1.0$ are also plotted for reference.

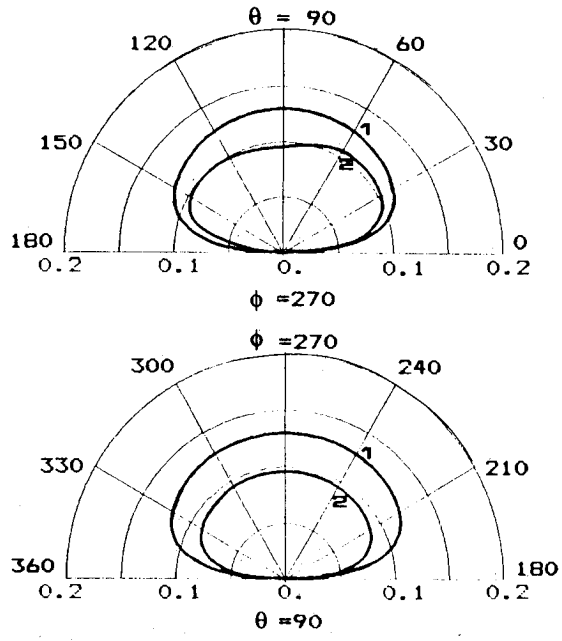

Fig. 9 Directional emittance for various positions on the edge surface: $n = 1.4$, $\omega = 0.99$, $2c = 5.0$; curve 1 for points at $z = c$, curve 2 for points at $z = 2c - 0.15$.

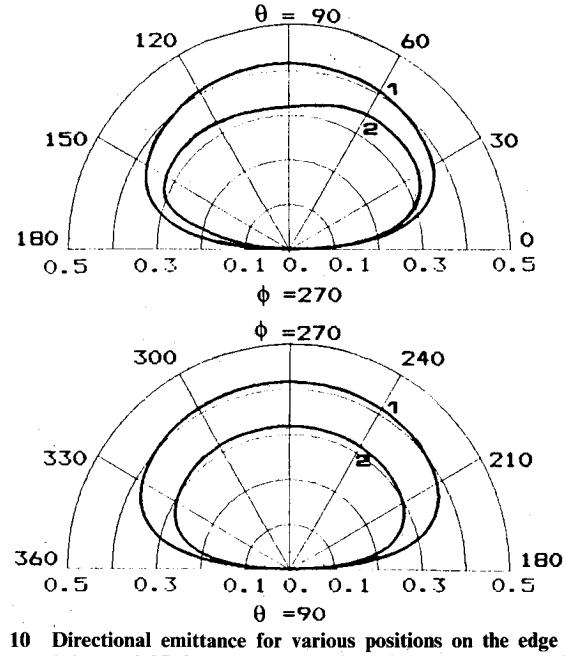

Fig. 10 Directional emittance for various positions on the edge surface: $n = 1.4$, $\omega = 0.95$, $2c = 5.0$; curve 1 for points at $z = c$, curve 2 for points at $z = 2c - 0.15$.

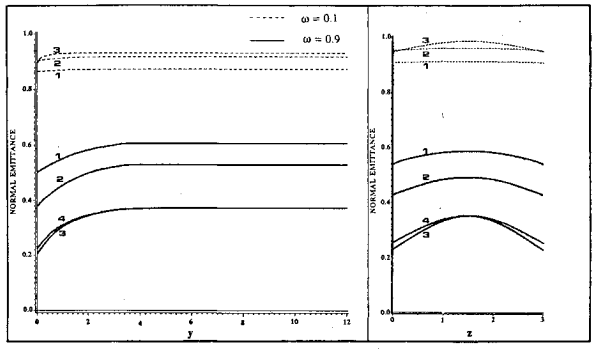

a) Top surface b) Edge surface

Fig. 11 Normal emittance for various refractive indexes: $\omega = 0.1$ and 0.9, $2c = 3.0$; curve 1 for $n = 1.8$, curve 2 for $n = 1.4$, curve 3 for $n = 1.0$ (Bobco), curve 4 for $n = 1.0$ (Love and Turner).

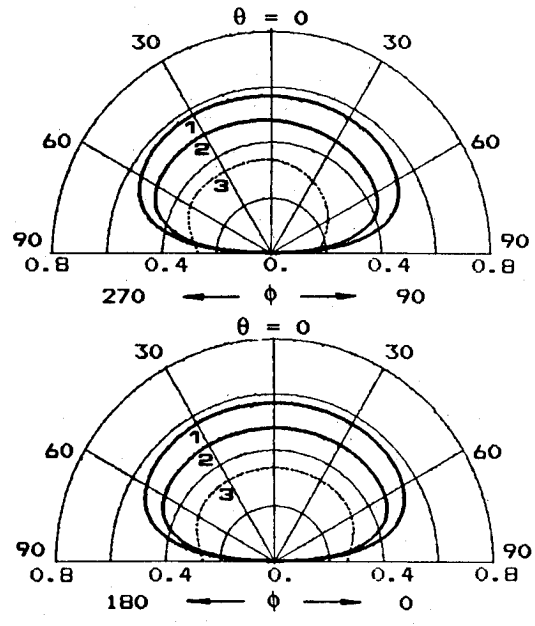

Fig. 12 Directional emittance from the edge surface at $z = 1.5$ for various refractive indexes: $\omega = 0.9$, $2c = 3.0$; curve 1 for $n = 1.8$, curve 2 for $n = 1.4$, curve 3 for $n = 1.0$ (Love and Turner).

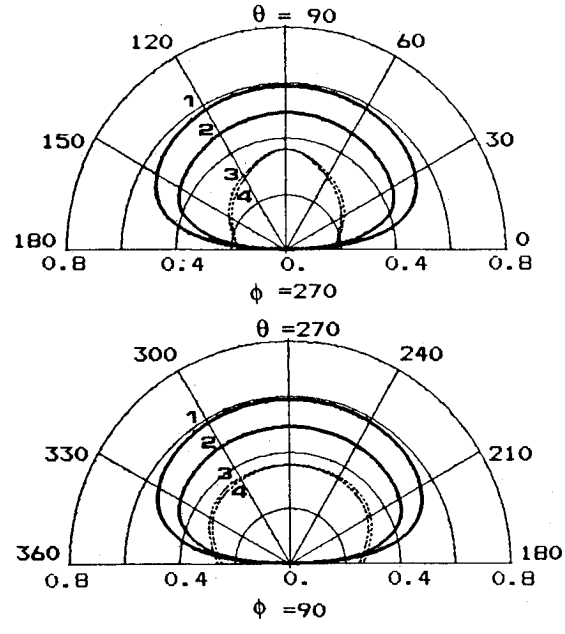

Fig. 13 Directional emittance from the edge surface at $y = 1.5$ for various refractive indexes: $\omega = 0.9$, $2c = 3.0$; curve 1 for $n = 1.8$, curve 2 for $n = 1.4$, curve 3 for $n = 1.0$ curve (Love and Turner), curve 4 for $n = 1.0$ (Bobco).

Conclusions

In conclusion, the complexity of formulation caused by the specular reflection was reduced by treating the images as effective media and by neglecting the radiation from faraway images. Then, the problem was described by an integral equation of the source function. The present work compares the solutions of the integral equation with the solutions by a Monte Carlo method and shows the formulation to be valid.

The resultant integral equation was solved by a successive iteration. The thermal radiation in the semi-infinite slab approaches that in an infinite slab at some distance away from the edge surface. This distance increases as the scattering albedo increases. The magnitude of directional emittance in a fixed direction increases as the point studied moves away from the edge surface. The dependence of plane directional emittance on azimuthal angle becomes stronger as the point

studied is located closer to the edge surface. A similar trend may be found for edge emittance. An increase of the refractive index reduces the emittance for a weakly scattering medium. For a strongly scattering medium, the reverse of the above is true. For a fixed refractive index, the directional emittance decreases as the albedo increases; however, the variation with albedos is less for smaller albedos. The directional emittance increases with the increase of the optical thickness.

References

[1]Bobco, R. P., "Directional Emissivities from a Two-Dimensional, Absorbing-Scattering Medium: the Semi-Infinite Slab," *Transactions of ASME Journal of Heat Transfer*, Vol. C89, 1967, pp. 313–320.

[2]Chu, C.-M. and Churchill, S. W., "Numerical Solution of Problems in Multiple Scattering of Electromagnetic Radiation," *Journal of Physical Chemistry*, Vol. 59, 1955, pp. 855–863.

[3]Crosbie, A. L. and Koewing, J. W., "Two-Dimensional Radiative Heat Transfer in a Planar Layer Bounded by Nonisothermal Walls," *AIAA Journal*, Vol. 17, 1979, pp. 196–203.

[4]Crosbie, A. L. and Linsenbardt, T. L., "Two-Dimensional Isotropic Scattering in a Semi-Infinite Medium," *Journal of Quantitative Spectroscopy and Radiative Transfer*, Vol. 19, 1978, pp. 257–284.

[5]Crosbie, A. L. and Schrenker, R. G., "Exact Expressions for Radiative Transfer in a Three-Dimensional Rectangular Geometry," *Journal of Quantitative Spectroscopy and Radiative Transfer*, Vol. 28, 1982, pp. 507–526.

[6]Crosbie, A. L. and Schrenker, R. G., "Radiative Transfer in a Two-Dimensional Rectangular Medium Exposed to Diffuse Radiation," *Journal of Quantitative Spectroscopy and Radiative Transfer*, Vol. 31, 1984, pp. 339–372.

[7]Crosbie, A. L. and Schrenker, R. G., "Multiple Scattering in a Two-Dimensional Rectangular Medium Exposed to Collimated Radiation," *Journal of Quantitative Spectroscopy and Radiative Transfer*, Vol. 33, 1985, pp. 101–125.

[8]Fiveland, W. A., "Discrete-Ordinates Solutions of the Radiative Transport Equation for Rectangular Enclosures," *Transactions of ASME Journal of Heat Transfer*, Vol. 106, 1985, pp. 699–706.

[9]Jefferies, J. T., "Radiative Transfer in Two Dimensions," *Optica Acta*, Vol. 2, 1955, pp. 163–167.

[10]Lewis, E. E., Miller, W. F., and Henry, T. P., "A Two-Dimensional Finite Element Method for Integral Neutron Transport Calculations," *Nuclear Science and Engineering*, Vol. 58, 1975, pp. 203–212.

[11]Lin, J.-D., "Directional Emittance from Isotropically Scattering Rectangular Media-Free and Reflecting Boundaries," Ph.D. Dissertation, Univ. of Oklahoma, Norman, 1985.

[12]Look, D. C., Jr. and Sundvold, P. D., "Anisotropic Two-Dimensional Scattering, Part II: Finite Depth and Refractive Index Effects," *AIAA Journal*, Vol. 22, 1984, pp. 571–573.

[13]Love, T. J. and Turner, W. D., "Directional Emittance from Emitting, Absorbing, and Scattering Media," *AIAA Progress in Astronautics and Aeronautics: Thermophysics: Applications to Thermal Design of Spacecraft*, Vol. 23, edited by J. T. Bevans, AIAA, New York, 1970, pp. 319–334.

[14]Modest, M. F. and Tabanfar, S., "A Multi-Dimensional Differential Approximation for Absorbing/Emitting and Anisotropically Scattering Media with Collimated Irradiation," *Journal of Quantitative Spectroscopy and Radiative Transfer*, Vol. 29, 1983, pp. 339–351.

[15]Noble, J. J., "The Zone Method: Explicit Matrix Relations for Total Exchange Areas," *International Journal of Heat and Mass Transfer*, Vol. 18, 1975, pp. 261–269.

[16]Ratzel, A. C. and Howell, J. R., "Two-Dimensional Radiation in Absorbing-Emitting-Scattering Media Using the P-N Appoximation," American Society of Mechanical Engineers Paper 82-HT-19, 1982.

[17]Smith, M. G., "The Transport Equation with Plane Symmetry and Isotropic Scattering," *Proceedings of the Cambridge Philosophical Society*, Vol. 60, 1964, pp. 909–921.

[18]Sutton, W. H., "Radiative Transfer in One and Two Dimensional Participating Media with Rectangular Coordinates," Ph.D. Dissertation, North Carolina State Univ., Raleigh, 1981.

[19]Turner, W. D. and Love, T. J., "Directional Emittance of a Two-Dimensional Ceramic Coating," *AIAA Journal*, Vol. 9, 1971, pp. 1849–1853.

[20]Wu, C. Y., "Analysis of Thermal Radiation in a Rectangular Scattering Medium with Fresnel Boundaries," Ph.D. Dissertation, Univ. of Oklahoma, Norman, 1986.

[21]Yuen, W. W. and Ho, C. F., "Analysis of Two-Dimensional Radiative Heat Transfer in a Gray Medium with Internal Heat Generation," *International Journal of Heat and Mass Transfer*, Vol. 28, 1985, pp. 17–23.

[22]Yuen, W. W. and Wong, L. W., "Analysis of Radiative Equilibrium in a Rectangular Enclosure with Gray Medium," *Transactions of ASME Journal of Heat Transfer*, Vol. 106, 1984, pp. 433–440.

[23]Armaly, B. F., "Influence of Refractive Index on Emittance: Finite Medium," *AIAA Progress in Astronautics and Aeronautics: Heat Transfer and Thermal Control Systems*, Vol. 60, edited by L. S. Fletcher, AIAA, New York, 1978, pp. 151–190.

[24]Armaly, B. F. and Lam, T. T., "Influence of Refractive Index on Reflectance from a Semi-Infinite Absorbing-Scattering Medium with Collimated Incident Radiation," *International Journal of Heat and Mass Transfer*, Vol. 18, 1975, pp. 893–900.

[25]Armaly, B. F., Lam, T. T., and Crosbie, A. L., "Emittance of Semi-Infinite Absorbing and Isotropically Scattering Medium with Refractive Index Greater than Unity," *AIAA Journal*, Vol. 11, 1973, pp. 1498–1502.

[26]Crosbie, A. L., "Emittance of Semi-Infinite Scattering Medium with Refractive Index Greater than Unity," *AIAA Journal*, Vol. 17, 1979, pp. 117–120.

[27]Crosbie, A. L., "Emittance of a Finite Scattering Medium with Refractive Index Greater than Unity," *AIAA Journal*, Vol. 18, 1980, pp. 730–732.

[28]Love, T. J., *Radiative Heat Transfer*, Charles Merrill Publishing, Columbus, OH, 1968.